

On-the-fly reduction of kinetic mechanisms using element flux analysis

Kaiyuan He, Ioannis P. Androulakis, Marianthi G. Ierapetritou *

Department of Chemical and Biochemical Engineering, Rutgers, The State University of New Jersey, Piscataway, NJ 08854, USA

ARTICLE INFO

Article history:

Received 2 October 2008

Received in revised form

25 September 2009

Accepted 29 September 2009

Available online 6 October 2009

Keywords:

On-the-fly reduction

Element flux analysis

Combustion

Dynamic simulation

Fuel

Model reduction

ABSTRACT

A systematic approach for on-the-fly mechanism reduction is proposed in this paper. The approach consists of element flux analysis and dynamic generation of reduced mechanisms during reactive flow computation. At each time step of the computation, a reduced mechanism is generated based on local conditions and no previous information or analysis is necessary. The approach is demonstrated in a plug-flow reactor (PFR) model and a pairwise mixing stirred reactor (PMSR) model. A detailed n-pentane oxidation mechanism with 385 species and 1895 elementary reactions and a primary reference fuel (PRF) mechanism with 1034 species and 4236 reactions are used to illustrate the proposed approach. Auto-ignition delay, temperature, and species composition profile predicted by the on-the-fly reduction scheme agree with the detailed simulation and experimental results over a wide range of temperatures and equivalence ratios.

© 2009 Elsevier Ltd. All rights reserved.

1. Introduction

In the past few decades, the increase in computational capability has contributed significantly towards the development of more accurate reactive flow simulations. This requires advances in both computational fluid dynamics (CFD) and chemical kinetic modeling. For chemical processes such as combustion and pyrolysis, detailed fundamental kinetic models consisting of hundreds of species and thousands of reactions have been developed (Curran et al., 1998; Faravelli et al., 2001; Granata et al., 2002; Lindstedt and Meyer, 2003). In practice, however, the incorporation of detailed kinetic mechanisms within complex CFD calculations is often infeasible due to extremely long CPU time required. Furthermore, the integration of detailed kinetic mechanisms in CFD models induces substantial differences in the species evolution time scales because of their vastly distinct reactivity. The resulting stiff ODE system renders the simulation even more expensive.

To alleviate the computational complexity while still retain good accuracy, great efforts have been devoted to the development of systematic methodologies that can effectively and efficiently reduce kinetic mechanism. Mechanism reduction rationales can be divided into three main categories: (1) Tabulation methods; where reactive propensity and corresponding system status are stored in forms of tabulated entries. Typical tabulation methods include in situ adaptive tabulation

(ISAT) (Pope, 1997) and intrinsic low dimensional manifolds (ILDM) (Mass and Pope, 1992). (2) Identification of redundancy. Species and reactions that can be removed from the mechanism without inducing significant errors are considered as redundant. Kuo and Wei (1969) proposed a lumping approach, which lumps concentrations of chemical species into a reduced species set. Other approaches aiming at identifying redundant species and reactions include sensitivity analysis proposed by Turanyi (1990) and Rabitz et al. (1983), optimization-based approaches proposed in (Androulakis, 2000; Bhattacharjee et al., 2003; Petzold and Zhu, 1999), DRG method proposed by Lu and Law (2005), a dynamic adaptive approach developed by Liang et al. (2008), and flux graph-based reduction approach proposed by Androulakis et al. (2004). (3) Time-scale decoupling methods; which is to decouple species and reactions with different time scales. Good examples are quasi steady state approximation (QSSA) (Peters, 1988), augmented reduced mechanism (ARM) generation (Chen, 1988), computational singular perturbation (CSP) (Lam and Goussis, 1994; Lu et al., 2001), and nonlinear perturbation methods (Kaper and Kaper, 2002; Tomlin et al., 1994).

The on-the-fly reduction scheme proposed in the current work lies in the second category: identification of redundancy. In the proposed approach, redundant species and reactions are identified efficiently and dynamically during the simulation. Reduced mechanisms are developed at each time step of the simulation, offering locally accurate chemistry representation. The proposed reduction technique is based on element flux analysis, which was first introduced by Revel et al. (1994) and implemented in mechanism reduction by Androulakis et al.

* Corresponding author. Tel.: +1 732 445 2971; fax: +1 732 445 2421.
E-mail address: marianth@sol.rutgers.edu (M.G. Ierapetritou).

(2004). The atomic fluxes for each atom (C, H, O, N, etc.) between sources and sinks are sorted in descending order. A user-selected cutoff is then applied on the flux list and source-sink pairs above the cutoff are included in the reduced mechanism. The main advantages of this approach are (a) no prior analysis or information is needed, and the approach can be applied to any condition encountered in the reactive flow simulation; and (b) the active species can be identified effectively without extensive computational overhead.

In the next section, the definition of element flux analysis and mechanism reduction is introduced, followed by the introduction of integrating the proposed reduction scheme in flow simulations. In Section 4, the methodology is demonstrated on a detailed n-pentane oxidation mechanism with 385 species and 1895 elementary reactions (Curran et al., 1998) and a detailed primary reference fuel (PRF) mechanism with 1034 species and 4236 (Curran et al., 1998) reactions in a pairwise mixing stirred reactor (PMSR) model (Pope, 1997) to assess the significant computational savings and a plug-flow reactor (PFR) model to assess the ability of the on-the-fly scheme to predict auto-ignition delays. Discussions of the results are presented in Section 5.

2. Element flux analysis and mechanism reduction

The element flux analysis, first introduced by Revel et al. (1994), provides a pointer to quantify the activity of species in a reaction system. The instantaneous elemental flux of atom A from species j to species k through reaction i , denoted as \dot{A}_{ijk} , is defined in Eq. (1). The total instantaneous flux between species j and k can be calculated by summing \dot{A}_{ijk} over all the reactions in which species j and k are involved, as represented in Eq. (2).

$$\dot{A}_{ijk}(t) = q_i(t) \frac{n_{A,j}n_{A,k}}{N_{A,i}} \quad (1)$$

$$\bar{A}_{jk}(t) = \sum_{i=1}^{N_R} \dot{A}_{ijk}(t) \quad (2)$$

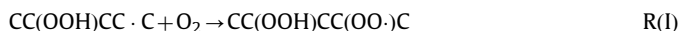
where $q_i(t)$ is instantaneous rate of reaction i (mol/s), $n_{A,j}$ is the number of atoms A in species j , $n_{A,k}$ is the number of atoms A in species k , $N_{A,i}$ is the total number of atoms A in reaction i , and N_R represents the number of reactions that these species participate as reactants or products. The atomic fluxes for different elements (C, H, O, and N) are quantified based on reaction rates at every time step using Eqs. (1) and (2) and sorted in descending order; active source-sink pairs can be identified by applying a user-selected cutoff value on the atomic flux. Since the chemical reacting system studied in the present work is hydrocarbon oxidation, it is reasonable to identify active species using carbon flux analysis. The active species identified by applying a cutoff on the carbon flux describe a large portion of the carbon transitions in the system.

However, in our previous study (He et al., 2008) it was found that Eqs. (1) and (2) may underestimate element flux for quasi-steady-state species induced by partial equilibrium reactions. This is due to the fact that partial equilibrium reactions have small net reaction rates compared to forward and reverse reaction rates. Therefore, flux pointer \dot{A}_{ijk} calculated through Eq. (1) is small although very fast element transition is taking place between species j and k through reaction i . To avoid miscalculating element flux for quasi-steady-state species induced by partial equilibrium reactions, both the forward and reverse reactions rates should be taken into account separately when calculating flux. Eq. (1) has

been modified as Eq. (3):

$$\dot{A}_{ijk}(t) = (|q_{ifwd}(t)| + |q_{irev}(t)|) \frac{n_{A,j}n_{A,k}}{N_{A,i}} \quad (3)$$

where q_{ifwd} and q_{irev} are the reactions rates of forward and reverse reactions, respectively. The absolute values of both forward and reverse reaction rates are used in Eq. (3) to avoid possible information loss for partial equilibrium reactions and quasi-steady-state species. Taking reaction $R(1)$ from n-pentane oxidation mechanism for example, the net reaction rate is 1.16×10^{-4} (mol/cm³s) while forward and reverse reaction rates are 1.7235×10^{-2} (mol/cm³s) and 1.7119×10^{-2} (mol/cm³s), respectively. CC(OOH)CC(OO·)C (C₅H₁₀OOH2-4O₂) then isomerizes and decomposes to form two OH radicals, thus it plays a crucial role in chain branching. However, if the carbon flux between species CC(OOH)CC(OO·)C (C₅H₁₀OOH2-4O₂) and CC(OOH)CC·C (C₅H₁₀OOH2-4) is calculated through Eq. (1), one will get 2.9×10^{-4} , which is much smaller than 8.59×10^{-2} as calculated through Eq. (3). The flux calculated by Eq. (3) will give species pair CC(OOH)CC(OO·)C (C₅H₁₀OOH2-4O₂) and CC(OOH)CC·C (C₅H₁₀OOH2-4) higher rank, thus crucial intermediate species CC(OOH)CC(OO·)C (C₅H₁₀OOH2-4O₂) has a greater chance to be retained in the reduced mechanism.



To better illustrate the proposed reduction scheme, let's for example examine three snapshots of n-pentane oxidation system which are taken under high temperature (1100 K), medium temperature (900 K), and low temperature (600 K) oxidation, respectively. Tables 1–3 summarize the results of flux analysis at these three conditions. Only a small portion of all 1954 source-sink pairs are shown in Tables 1–3 due to the extensive length of the entire list. The cumulative weight is calculated by dividing the cumulative flux sum by the total flux at current time step. The indicator represents the portion of total carbon flux captured by the source-sinks above this level. In Table 1, flux values summarize the system at the initial stage of low-temperature (600 K, stoichiometric) n-pentane oxidation. At low temperature, oxygen adds to the amyl radicals forming amylperoxy radicals (Table 1-line1), and the peroxy radicals isomerize by hydrogen atom transfer to hydroperoxide-amyl radicals (Table 1-line7). The hydroperoxide-amyl radicals then react with a second oxygen (Table 1-line8), undergoes similar isomerization (Table 1-line9), and decompose through chain branching pathway (Table 1-line15 and line23). This second oxygen addition and chain branching pathway is responsible for the increase of oxidation rate that leads to low temperature oxidation and cool flame formation. The characteristic low-temperature pathways are well represented by the active source-sinks summarized in Table 1.

As temperature increases, the second oxygen addition pathway becomes less favorable while the decomposition of the initial hydroperoxide-amyl radicals dominates the system. This pathway shift is reflected by the active source-sink pairs in Table 2, which summarizes the medium temperature (900 K) oxidation of n-pentane. The first oxygen adds to the amyl radical forming an amylperoxy radical (Table 2-line7), and isomerizes by hydrogen atom transfer to a hydroperoxide-amyl radical (Table 2-line10). Then the hydroperoxide-amyl radical decomposes to olefin (Table 2-line11), instead of adding a second oxygen. The decomposition pathway of the hydroperoxide-amyl radical only generates one ·OOH instead of two ·OH in the second oxygen addition pathway. This pathway shift slows the oxidation rate even when temperature increases, which is the phenomenon known as negative temperature coefficient (NTC).

When the system temperature increases further, even the first oxygen addition becomes less favorable. The β-scission of

Table 1

Flux analysis of system snapshot at the initial stage of n-pentane low temperature oxidation.

Index	Sources	Sinks	Instantaneous carbon flux	Cumulative flux sum	Cumulative weight (%)
1	C5H11-2	C5H11O2-2	4.896	4.896	7.94
2	NC5H12	C5H11-2	4.855	9.751	15.82
3	C5H11-3	C5H11O2-3	2.439	12.190	19.78
4	NC5H12	C5H11-3	2.418	14.607	23.70
5	C5H11-1	C5H11O2-1	2.388	16.995	27.58
6	NC5H12	C5H11-1	2.385	19.380	31.45
7	C5H11O2-2	C5H100OH2-4	2.246	21.626	35.09
8	C5H100OH2-4	C5H100OH2-4O2	2.239	23.866	38.73
9	C5H100OH2-4O2	NC5KET24	2.213	26.079	42.32
⋮					
15	NC5KET24	CH3COCH2	1.085	33.243	53.94
16	CH3COCH2O2	CH3COCH2O2H	1.045	34.287	55.64
17	C5H11O2-3	C5H11O-3	0.963	35.250	57.20
18	C5H11O2-1	C5H100OH1-3	0.942	36.192	58.73
19	C5H100OH1-3	C5H100OH1-3O2	0.935	37.126	60.24
20	C5H11O-3	C2H5CHO	0.928	38.055	61.75
21	C5H100OH1-3O2	NC5KET13	0.869	38.924	63.16
22	C5H11O-2	CH3CHO	0.789	39.713	64.44
23	NC5KET24	CH3CHO	0.723	40.436	65.62
⋮					
69	C5H100OH1-4	C5H100OH1-4O2	0.177	55.161	89.51
70	C2H5	C2H4	0.173	55.334	89.79
71	C5H11O2-3	C5H11O-2	0.172	55.506	90.07
⋮					
140	PC4H9O2H	PC4H9O	0.035	60.970	98.94
141	C2H5COCH2	C2H5COCH3	0.034	61.004	98.99
142	CH3CHO	CH3CO	0.033	61.037	99.04
⋮					
			Total Flux	61.626	

The first two columns represent the sources and sinks. The third column is the instantaneous carbon flux between the two species, which are sorted in descending order. The fourth column is the cumulative sum of flux up to this depth on the list. The fifth column is the cumulative weight calculated by dividing the cumulative flux sum by the total flux of the system at this time step. Same structure for Tables 2 and 3.

Table 2

Flux analysis of system snapshot at the initial stage of n-pentane medium temperature oxidation.

Index	Sources	Sinks	Instantaneous carbon flux	Cumulative flux sum	Cumulative weight (%)
1	NC5H12	C5H11-2	28.828	28.828	11.86
2	C5H11-2	C3H6	15.793	44.621	18.36
3	NC5H12	C5H11-3	14.371	58.992	24.27
4	NC5H12	C5H11-1	14.367	73.359	30.18
5	C5H11-2	C2H5	10.528	83.887	34.51
6	C2H5	C2H4	7.314	91.201	37.52
7	C5H11-3	C5H11O2-3	6.949	98.150	40.38
8	C5H11-3	C4H8-1	6.035	104.185	42.87
9	C5H11-1	C5H11O2-1	5.763	109.948	45.24
10	C5H11O2-3	C5H100OH3-2	4.993	114.941	47.29
11	C5H100OH3-2	C5H10-2	4.924	119.866	49.32
12	C3H6	IC3H7	4.582	124.447	51.20
13	C5H11-1	NC3H7	4.376	128.823	53.00
14	C5H11-2	C5H11O2-2	4.164	132.987	54.72
15	HCO	CO	3.404	136.391	56.12
16	C5H11-1	C2H4	2.917	139.308	57.32
17	CH3O	CH2O	2.907	142.215	58.51
18	C5H11O2-1	C5H100OH1-3	2.619	144.834	59.59
19	C2H5	C2H5O	2.582	147.416	60.65
20	C5H11O2-2	C5H100OH2-4	2.416	149.833	61.65
21	C5H10-2	C5H9	2.237	152.069	62.57
22	IC3H7	IC3H7O2	2.188	154.258	63.47
23	NC3H7	NC3H7O2	2.104	156.362	64.33
24	CH2O	HCO	2.062	158.424	65.18
25	C3H6	C3H5-A	2.056	160.479	66.03
26	C2H5	C2H5O2	2.007	162.486	66.85
27	C5H100OH1-3	C5H1001-3	1.971	164.457	67.66
⋮					
			Total Flux	243.053	

amyl radicals dominates the system, which defines the high temperature oxidation. Table 3, which summarizes the high temperature (1100 K) oxidation of n-pentane, includes

crucial species on the β -scission pathway: amyl radicals decompose directly to smaller alkyl radicals instead of reacting with oxygen.

Table 3
Flux analysis of system snapshot at the initial stage of n-pentane high temperature oxidation.

Index	Sources	Sinks	Instantaneous carbon flux	Cumulative flux sum	Cumulative weight (%)
1	NC5H12	C5H11-2	650.45	650.45	11.15
2	C5H11-2	C3H6	406.92	1057.37	18.13
3	NC5H12	C5H11-1	327.23	1384.60	23.74
4	NC5H12	C5H11-3	324.52	1709.12	29.30
5	C5H11-2	C2H5	271.28	1980.40	33.95
6	C5H11-3	C4H8-1	248.15	2228.55	38.21
7	C5H11-1	NC3H7	173.05	2401.60	41.18
8	C3H6	IC3H7	168.89	2570.49	44.07
9	HCO	CO	160.02	2730.51	46.81
10	C3H6	C3H5-A	146.96	2877.47	49.33
11	C2H5	C2H4	135.89	3013.36	51.66
12	C4H8-1	C4H7	129.93	3143.29	53.89
13	C2H5	C2H5O	124.65	3267.94	56.03
14	NC3H7	C2H4	120.56	3388.50	58.10
15	C5H11-1	C2H4	115.37	3503.87	60.07
16	CH2O	HCO	110.89	3614.76	61.98
17	C3H5-A	C3H5O	101.01	3715.77	63.71
18	CH3O	CH2O	84.61	3800.38	65.16
19	C3H5O	C2H3CHO	72.93	3873.31	66.41
20	CH3	CH3O	68.51	3941.82	67.58
21	C5H11-3	CH3	62.04	4003.86	68.65
22	NC3H7	CH3	60.28	4064.14	69.68
23	C2H5O	CH3CHO	58.56	4122.70	70.68
...					
			Total Flux	5832.59	

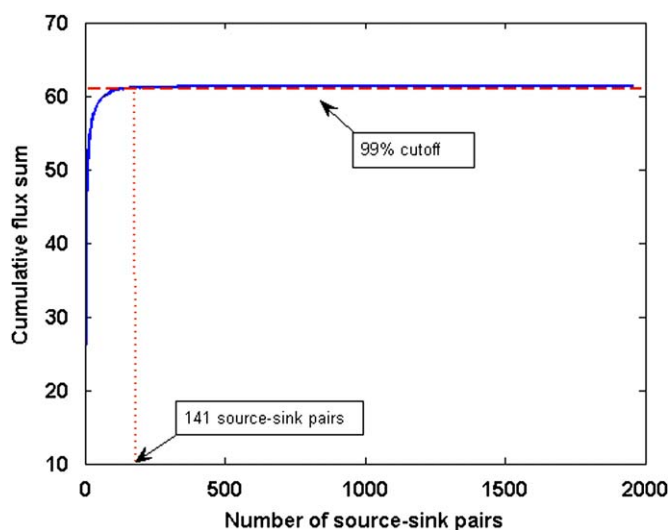


Fig. 1. Cumulative flux sum distribution pattern of n-pentane combustion system. Detailed mechanisms: 385 species and 1895 reactions. Total number of source-sink pairs: 1954.

As shown in Tables 1–3, a small portion of source-sink pairs can capture most of the carbon flux. This is due to the fact that at certain phase of a combustion process, only part of the entire pathway is active while the rest has little or no activity. As the combustion process evolves, different part of the pathways become active. For example, at the initial phase, decomposition of the fuel has the highest activity; at the intermediate phase, large hydrocarbons decompose further to smaller hydrocarbons and radicals; and at the final phase of the combustion, small molecules oxidized to CO_2 is the most active. To illustrate the flux distribution pattern, cumulative flux sum of Table 1 was plotted versus number of species pairs in Fig. 1. As shown in the cumulative flux sum distribution, 99% of the carbon flux at

current step is allocated in 141 source-sink pairs (out of 1954 pairs in total). The rest more than 90% source-sink pairs only comprise 1% of the total carbon flux. Flux data at other conditions was sampled and similar distribution pattern was observed. Thus it is reasonable to use the top few source-sinks to describe the system at that particular time point while the rest of the source-sinks are considered to be of trivial importance at current step. By setting a high percentage cutoff, it is also ensured that those species involved in slow reactions at current phase are also included, even relatively lower rank was designated to them. This is because those species that do not belong to current phase will have the lowest rank and will be eliminated in the reduced mechanism. However, as the system evolves, different set of source-sink pairs will become active. Thus our methodology is designed to update the mechanism dynamically during the simulation, which will be discussed in details in the following section.

3. On-the-fly reduction framework

Given the mechanism reduction method based on flux analysis, the next step is to integrate the reduction scheme in reactive flow simulation. The reactive flow models typically span a broad range of conditions such as species concentrations, temperature and pressure. To develop locally accurate reduced mechanisms for different reactive conditions, we propose an on-the-fly scheme, which updates reduced mechanisms dynamically as the condition changes. The entire on-the-fly reduction framework is summarized in Fig. 2. Reactive flow models usually divide the simulation into discrete time steps. During each step, both the reaction and the mixing effect are taken into account. The idea of on-the-fly reduction scheme is to generate a reduced mechanism for each time step. Compared to adaptive reduction schemes, which construct a library of reduced mechanisms *a priori* and assume the union of feasible regions of these mechanisms covers the entire condition space encountered in the simulation, the main advantage of dynamic mechanism generation is that,

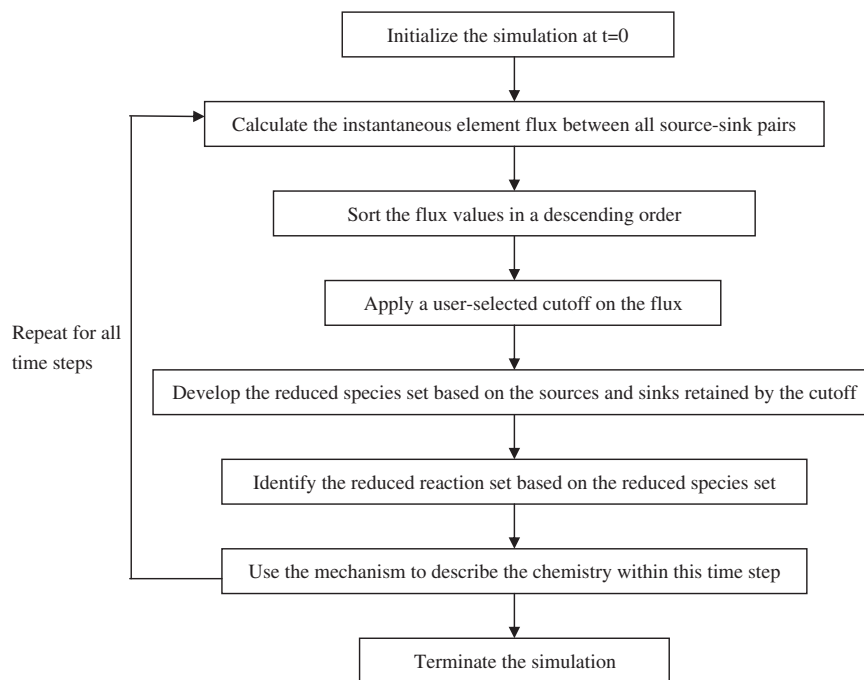


Fig. 2. Integration of the on-the-fly reduction scheme in the context of a reactor model.

accurate mechanisms can be developed based on local reactive conditions. Since a wide range of conditions might be encountered in reactive flow simulation, the priori library of reduced mechanisms may lose its validity at certain conditions that are out of its validity range. However, accurate reduced mechanisms can always be developed for any condition that is encountered in the flow simulation.

To integrate the reduction scheme with the reactive flow simulation, we analyze the carbon element flux at each time step and sort the source-sink pairs in a descending order. Then a user-selected cutoff value is applied on the flux and active sources and sinks characterized by high flux values are retained in the reduced mechanism while source-sink pairs below the cutoff are neglected. The union set of the species in the retained source-sink pairs comprises the species set. Based on the species set, a reaction is included in the reduced mechanism only if all its reactants and products are included in the species set; i.e., any reaction that involves species not included in the species set will be removed. The reduced mechanism is then integrated in CHEMKIN application (Kee et al., 1996). A flowchart of the integration of CHEMKIN and main function is represented in Fig. 3. ϕ_{ns}^k are concentrations of all ns species at k th iteration. $\phi_{ns'}^k$ are concentrations of ns' species in the reduced mechanism while $\phi_{(ns-ns')}^k$ are concentrations of $(ns-ns')$ species that are not included in the reduced mechanism. The species that are not included in the reduced mechanism are considered as dormant (to have zero production rates) at current time step. Their concentrations are kept unchanged in the main function and are not integrated in CHEMKIN application. As the system advances to the next time step, the flux analysis and reduction process are applied and a new reduced mechanism is generated.

4. Demonstration of the proposed methodology

To validate the feasibility and accuracy of the on-the-fly reduction approach, the reduction scheme is demonstrated in the context of a reactor model. Since the elemental flux analysis is

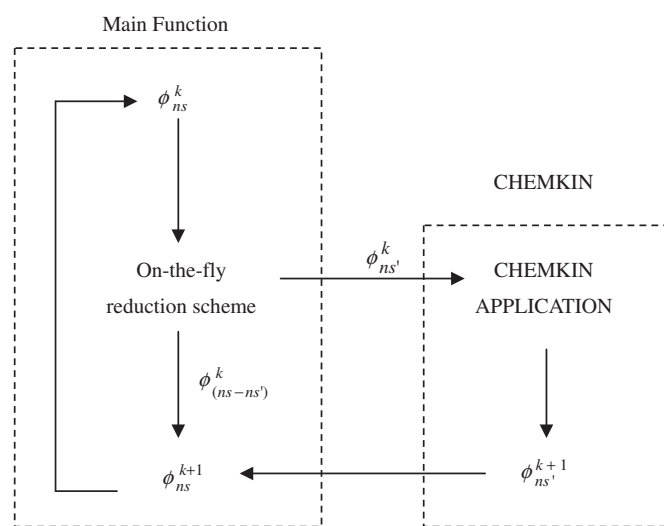


Fig. 3. Integration of CHEMKIN application in the main function and the on-the-fly reduction scheme.

performed based on the concentrations of all the species, the flow model should be able to track all the species present in the detailed mechanism, hence at any time step the species concentrations can be retrieved and thus flux analysis can be implemented. In the present work, a pairwise mixing stirred reactor (PMSR) (Pope, 1997) model and a plug-flow reactor (PFR) model are used to demonstrate the proposed methodology. These two zero-dimensional reactor models are used primarily because they are computational tractable even with detailed kinetic model, and covers a broad range of conditions in the composition space. These properties merit our research in two aspects: (a) the reactive flow simulation in both models can be solved with detailed kinetic mechanism to provide temperature and composition profiles which are used to evaluate the performance of the

on-the-fly reduction scheme; and (b) the PFR predicts autoignition delay which is considered as an important property of fuels and the stochastic pairing process in PMSR provides a wide range of reactive conditions to validate the on-the-fly reduction scheme.

4.1. Pairwise mixing stirred reactor

The pairwise mixing stirred reactor (PMSR) (Pope, 1997) model is first used to validate the methodology for the prediction of temperature and species compositions in the simulation. In a PMSR model reactive fluid composed of fuels, oxidizers, and diluents is modeled as even number of particles. The simulation is advanced in discrete time steps. At each time step, all the particles are randomly paired and the composition of each pair of particles undergoes a mixing-and-reaction evolution pattern, i.e., the composition first evolves through a mixing fractional time step followed by a reaction fractional time step. The microscale mixing of each pair of particles (say, p and q) and reaction fraction step are described by Eq. (4):

$$\begin{aligned} \frac{d\varphi^{(p)}}{dt} &= -(\varphi^{(p)} - \varphi^{(q)})/\tau_{mix} \\ \frac{d\varphi^{(q)}}{dt} &= -(\varphi^{(q)} - \varphi^{(p)})/\tau_{mix} \\ \frac{d\varphi^{(i)}}{dt} &= S(\varphi^{(i)}) \end{aligned} \quad (4)$$

where τ_{mix} is the mixing timescale, $\varphi^{(p)}$ and $\varphi^{(q)}$ are compositions of particle p and q , respectively. $S(\varphi^{(i)})$ are the creation or destruction rates of species due to chemical reactions. The random pairing feature of PMSR model mimics the imperfectly mixed nature of reactive flows at the molecular level. On the other hand, the stochastic nature of the model results in a wide range of the temperature and species composition space, thus providing a rigorous test bed for the proposed on-the-fly reduction scheme. The PMSR simulation is performed with 100 particles and 100 steps, and the time step is $\Delta t = 1 \times 10^{-2}$ s. The mixing time scale is $\tau_{mix} = 1 \times 10^{-1}$ s, the pairing time scale is $\tau_{pairing} = 1 \times 10^{-1}$ s, and the residence time scale is $\tau_{res} = 1.0$ s. The primary reference fuel oxidation mechanism established by Curran et al. (1998) are used in the analysis, and the thermo physical properties and reaction rate definitions are provided by CHEMKIN-II (Kee et al., 1996).

The PRF, a mixture of n-heptane and iso-octane, is used to define the octane number for gasoline. Octane number is the number which gives the volume percentage of iso-octane in a mixture of iso-octane and n-heptane, which would have the same anti-knocking capacity as the fully blended gasoline under consideration. The chemistry of PRF includes many of the features of large molecular-weight blended fuels. N-heptane is a reactive straight-chain paraffin while iso-octane is a less reactive branched-chain paraffin. At high temperatures, fuel decomposition reactions (β -scission) are the major pathways in the combustion process of each fuel, whereas at low temperatures, the addition of O_2 to alkyl radicals dominates the combustion chemistry. Both low- and high-temperature regimes are important for fuels combustion process in spark-ignition (SI) and compression-ignition (CI) engines. To prove the validity of

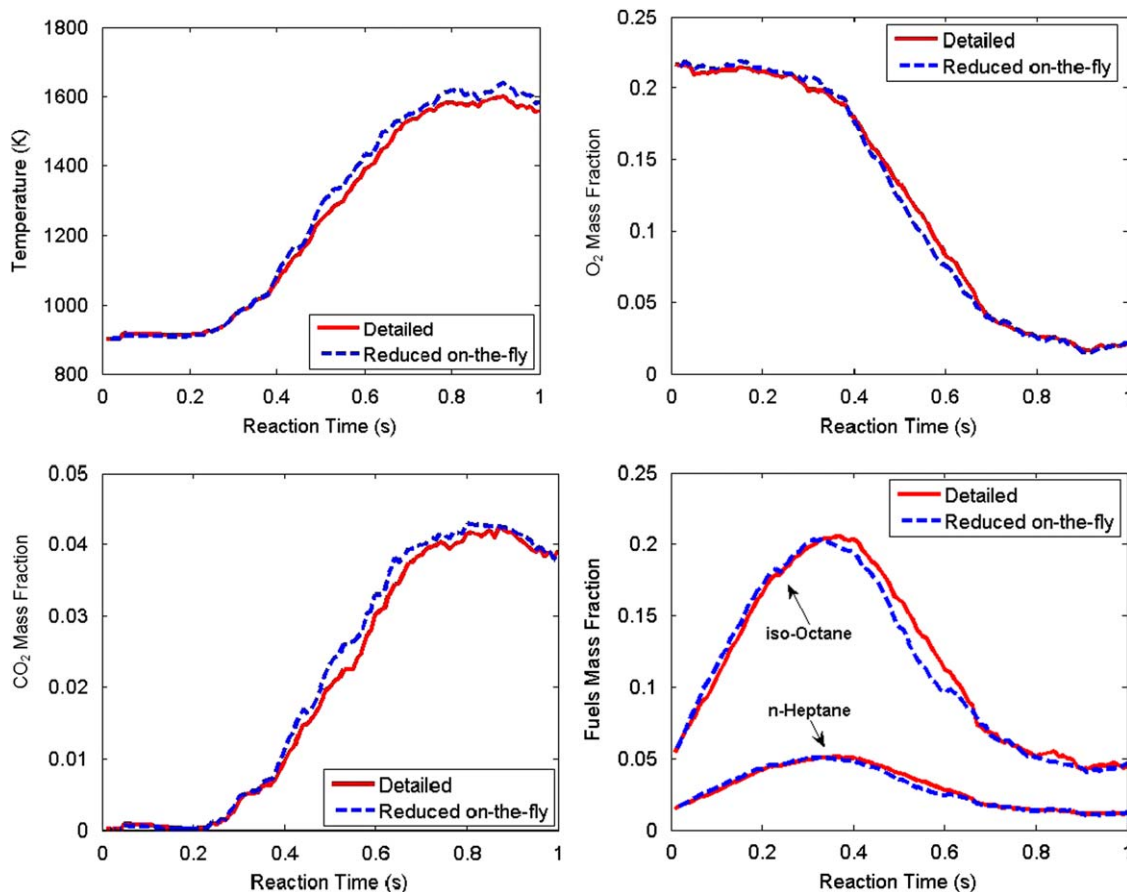


Fig. 4. On-the-fly scheme tested for PRF oxidation in PMSR. Initial conditions: $T=900$ K, $ON=80$, $y_{iso-octane}=0.050$, $y_{n-heptane}=0.012$, $y_{O_2}=0.219$, $y_{N_2}=0.719$.

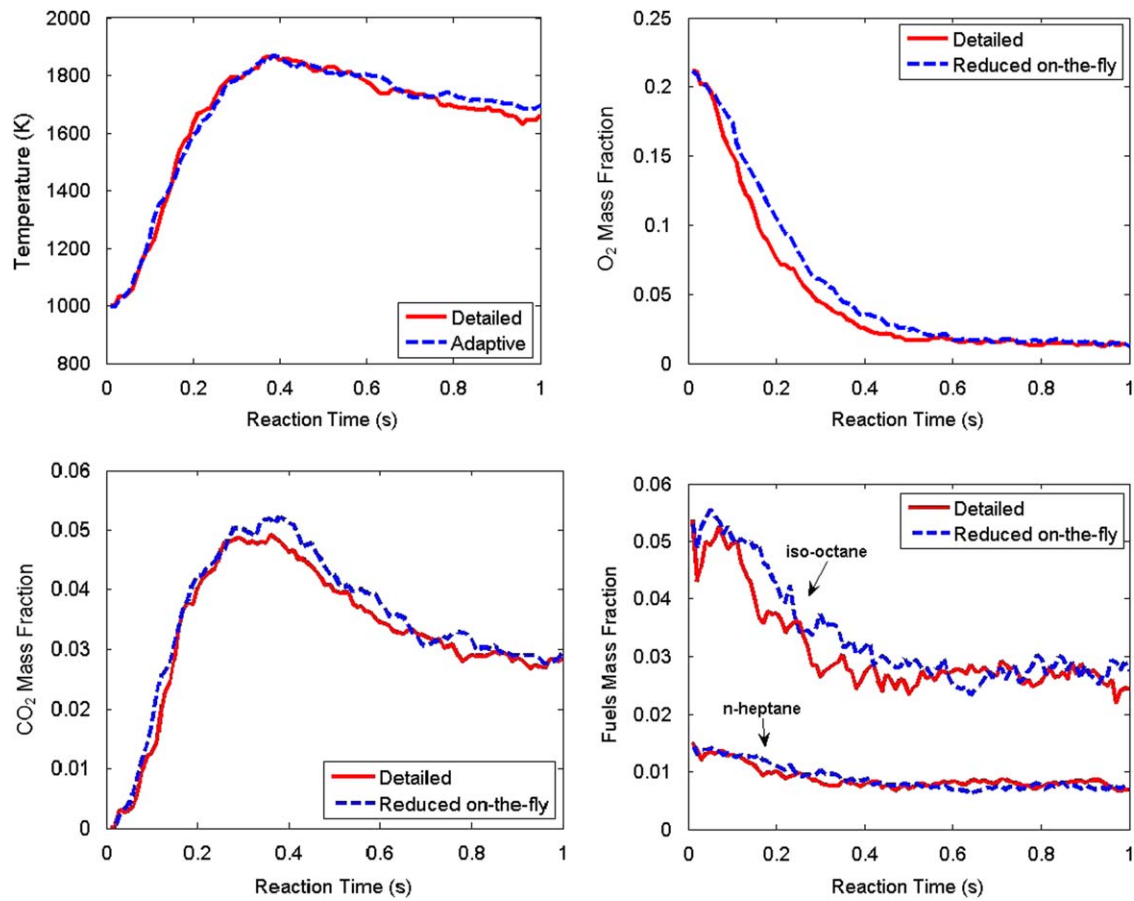


Fig. 5. On-the-fly scheme tested for PRF oxidation in PMSR. Initial conditions: $T=1000\text{ K}$, $ON=80$, $y_{\text{iso-octane}}=0.050$, $y_{\text{n-heptane}}=0.012$, $y_{\text{O}_2}=0.219$, $y_{\text{N}_2}=0.719$.

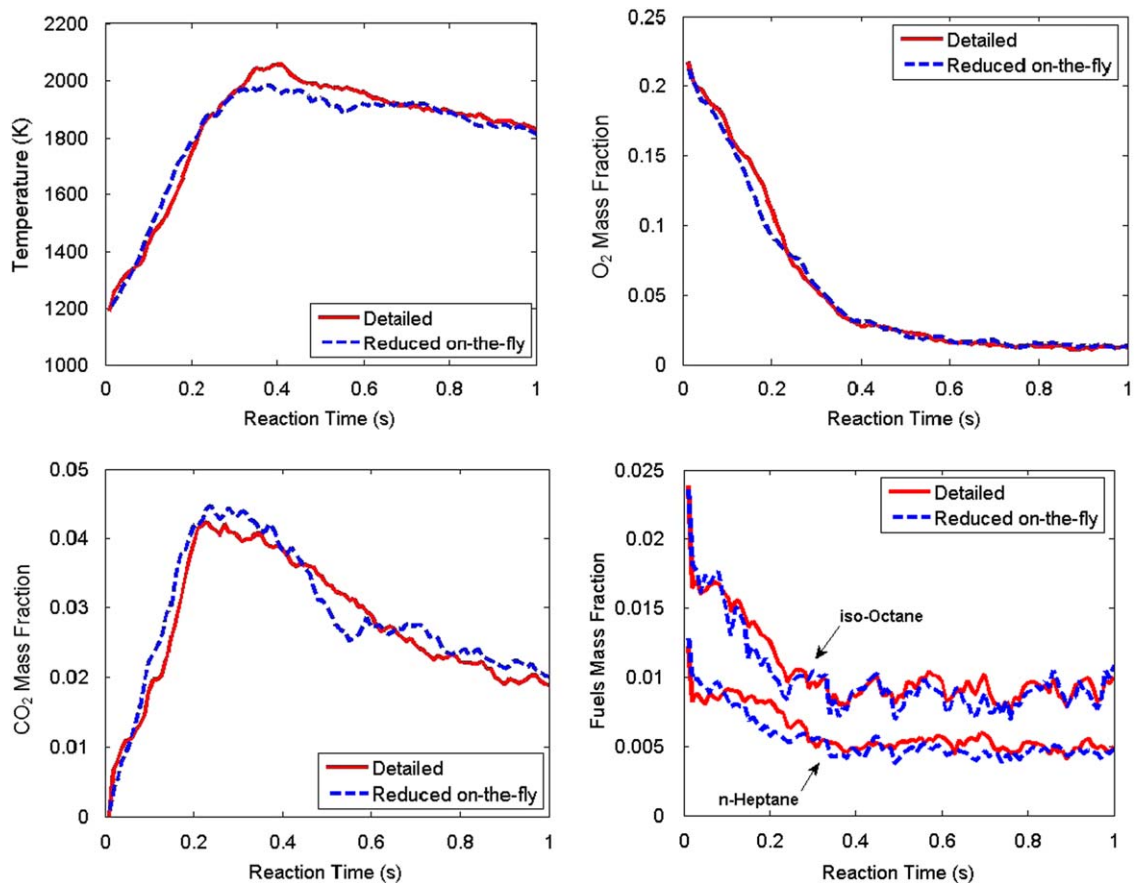


Fig. 6. On-the-fly scheme tested for PRF oxidation in PMSR. Initial conditions: $T=1200\text{ K}$, $ON=80$, $y_{\text{iso-octane}}=0.050$, $y_{\text{n-heptane}}=0.012$, $y_{\text{O}_2}=0.219$, $y_{\text{N}_2}=0.719$.

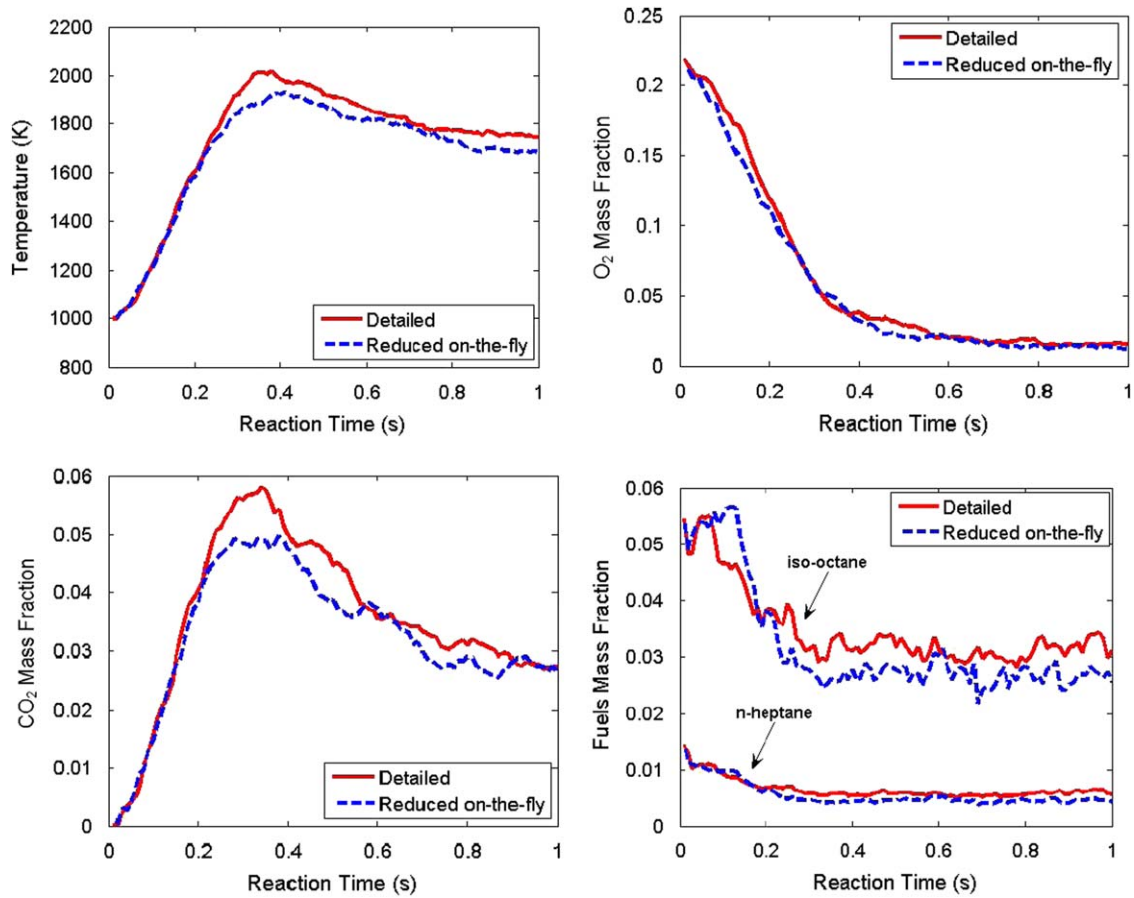


Fig. 7. On-the-fly scheme tested for PRF oxidation in PMSR. Initial conditions: $T=1000$ K, $ON=87$, $y_{\text{iso-octane}}=0.054$, $y_{\text{n-heptane}}=0.008$, $y_{\text{O}_2}=0.219$, $y_{\text{N}_2}=0.719$.

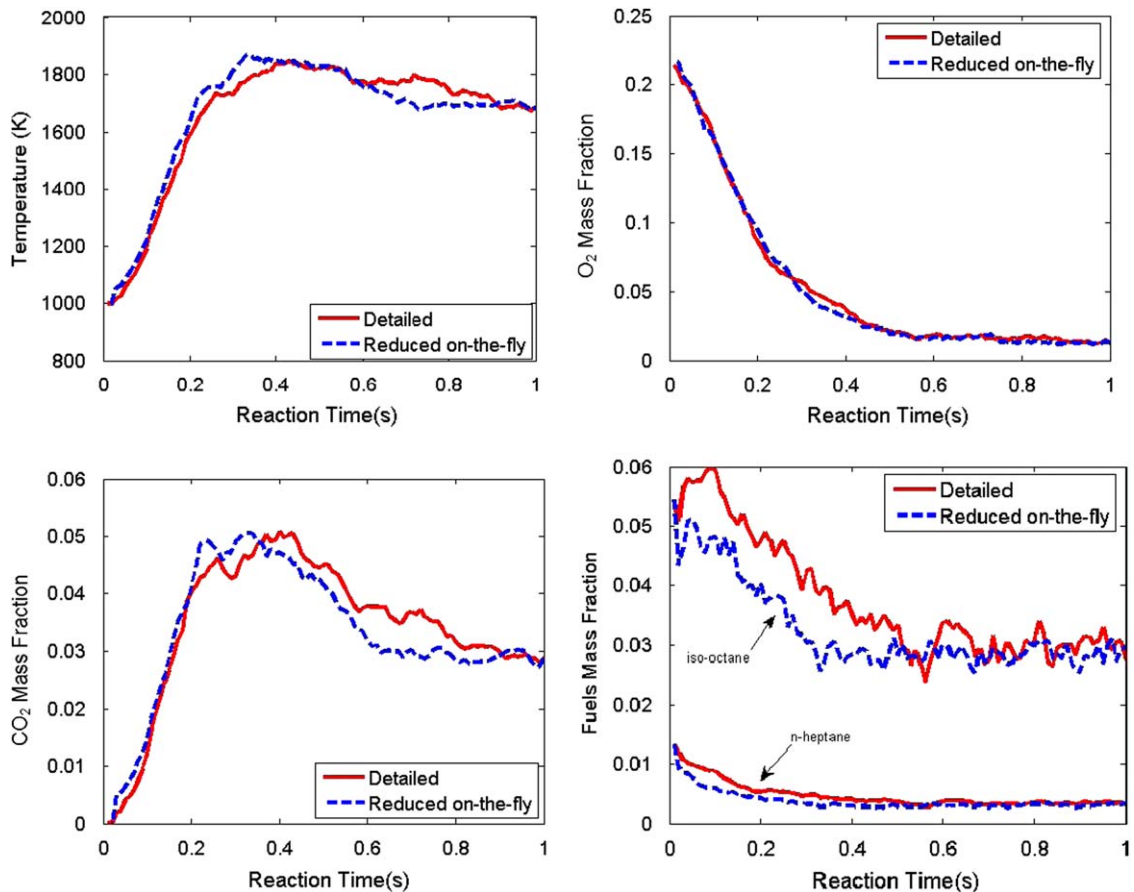


Fig. 8. On-the-fly scheme tested for PRF combustion in PMSR. Initial conditions: $T=1000$ K, $ON=92$, $y_{\text{iso-octane}}=0.057$, $y_{\text{n-heptane}}=0.005$, $y_{\text{O}_2}=0.219$, $y_{\text{N}_2}=0.719$.

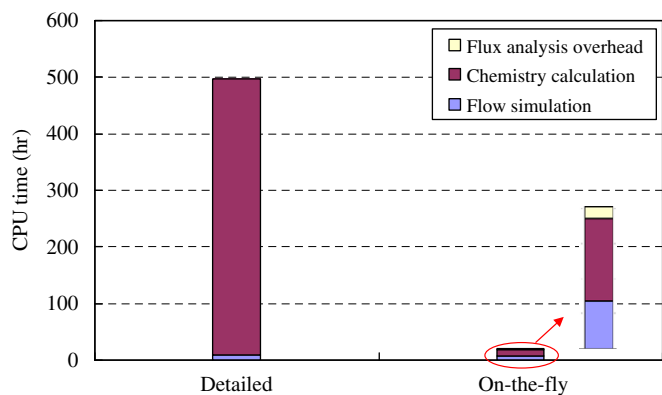


Fig. 9. CPU time of n-pentane combustion simulation in a PMSR model. Initial conditions: $T=900\text{ K}$, $ON=80$, $y_{\text{iso-octane}}=0.050$, $y_{\text{n-heptane}}=0.012$, $y_{\text{O}_2}=0.219$, $y_{\text{N}_2}=0.719$.

Table 4

CPU time of n-pentane combustion simulation in a PMSR model.

	Detailed (h)	On-the-fly (h)
Flow simulation	9.4	6.7
Chemistry calculation	487.0	11.9
Flux analysis overhead	0	1.7
Total	496.4	20.3

proposed methodology in complex chemistry simulations, the detailed PRF mechanism consisting 1034 species and 4236 reactions is used in PMSR. Different initial temperatures 900, 1000 and 1200 K and different octane numbers ON80, ON87 and ON92 at 1000 K are tested using PMSR simulations. A 99% cutoff is used for the on-the-fly reduction scheme and the results are represented in Figs. 4–8. Due to the stochastic nature of the PMSR model, fluctuations were observed on temperature and species profiles. In order to cancel the fluctuation, the average results of 5 simulations were used for each condition. Since particles are randomly mixed in the PMSR simulation, a wide range of temperature and species composition space can be accessed. As a result, mechanisms developed for each particle vary dramatically. The average size of the reduced mechanisms in the entire simulation is 87 species and 475 reactions. Good agreement between reduction scheme and detailed simulation can be observed for different temperatures and ON's. CPU time of the detailed simulation and on-the-fly reduction scheme is represented in Fig. 9. The entire simulation is divided into three parts: flow simulation, chemistry calculation, and flux analysis overhead. Flow simulation includes all the mixing and transport calculations. Chemistry calculation involves kinetic equations and coupled ODE system. Flux calculation and mechanism generation is considered as overhead. CPU time on each part is listed in Table 4. As shown in Table 4, the on-the-fly reduction scheme reduced chemistry calculation by a factor of 40. Meanwhile, the overhead introduced by flux analysis comprises less than 10% of the total CPU time of the on-the-fly reduction scheme.

4.2. Demonstration in PFR

The on-the-fly reduction scheme is tested in an adiabatic plug-flow reactor (PFR) model to evaluate the performance in the prediction of autoignition delay of hydrocarbon oxidation. The

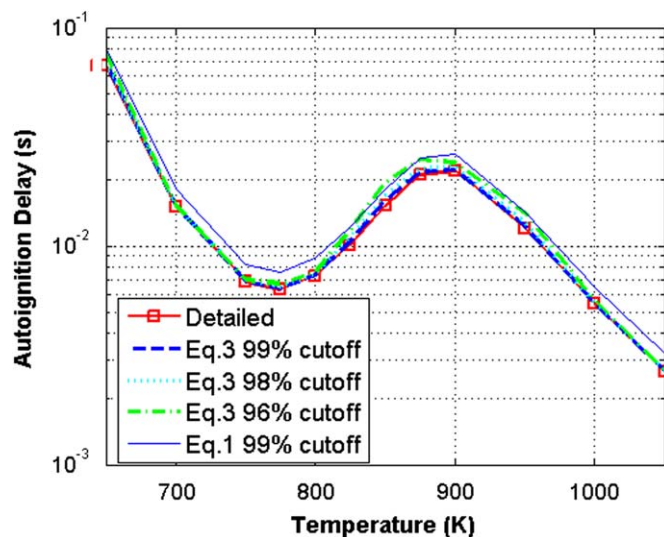


Fig. 10. Auto-ignition delays of n-pentane predicted by on-the-fly scheme in a PFR model. $\phi=1$, $P=8.4\text{ bar}$.

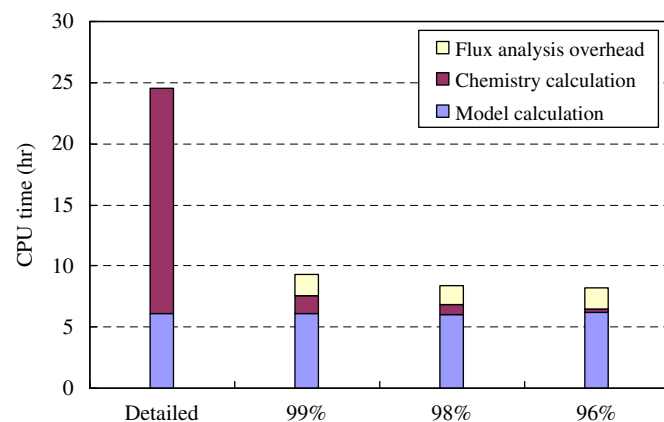


Fig. 11. CPU time of n-pentane combustion simulation in a PFR model. $\phi=1$, $P=8.4\text{ bar}$, $T=1000\text{ K}$.

Table 5

CPU time of n-pentane combustion simulation in a PFR model.

	On-the-fly			
	Detailed (min)	99% (min)	98% (min)	96% (min)
Model calculation	6.1	6.1	6.0	6.2
Chemistry calculation	18.4	1.5	0.8	0.3
Flux analysis overhead	0	1.7	1.6	1.7
Total	24.5	9.3	8.4	8.2
Mechanism size^a	385	102	83	54

^a Species number is used to represent mechanism size. For the on-the-fly scheme, average species number is used.

autoignition delay of n-pentane predicted by the on-the-fly scheme with different cutoff values are compared with detailed simulations in Fig. 10. Stoichiometric fuel/air mixture is used for all simulations. As shown in Fig. 10, longer autoignition delay has been observed when Eq. (1) is used to calculate flux. This is due to the fact that some quasi-steady state species induced by partial equilibrium reactions are given small flux by Eq. (1) and

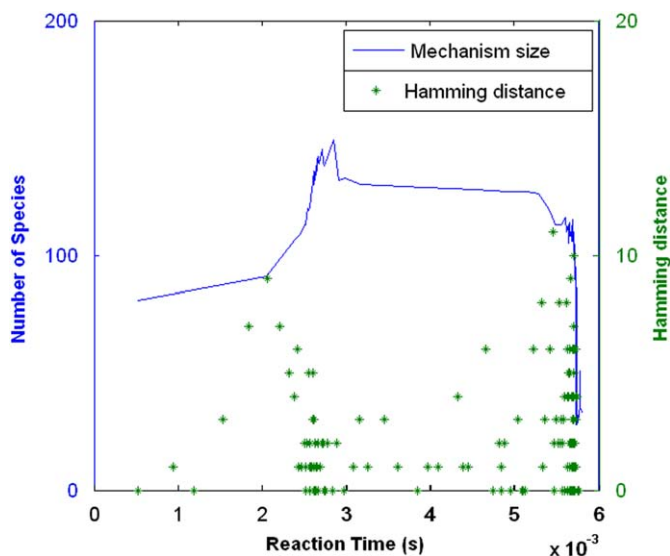


Fig. 12. Hamming distance between two consecutive mechanisms compared to the mechanism size (represented by the number of species) for the on-the-fly scheme of n-pentane combustion in a PFR model. $\phi=1$, $P=8.4$ bar, $T=1000$ K.

consequently eliminated in the reduced mechanism. It is also observed that results of higher cutoff values have smaller deviation from those of the detailed simulation. The CPU time of the detailed simulation and the on-the-fly reduction scheme using different cutoffs are represented in Fig. 11. The entire simulation is divided into three parts: model calculation, chemistry calculation, and flux analysis overhead. CPU time on each part is listed in Table 5. The PFR simulation takes 24.5 min even when detailed mechanism is used, thus the overall computational speed up is not as significant as gained in PMSR. However, the on-the-fly reduction scheme reduced CPU time on chemistry calculation by a factor of 12 when 99% cutoff was used. Another advantage of the on-the-fly scheme is that although the mechanism size varies for different stages of oxidation, the difference between two consecutive mechanisms is very small, which means that the reduced mechanism evolves smoothly as the reaction system advances. To quantitatively evaluate this observation, each reduced mechanism is represented as a binary vector with 385 dimensions. Each coordinate of the vector is a binary variable with 1 denoting the presence of the specie in the reduced mechanism and 0 the absence of the specie. Thus a particular combination of 385 binary variables represents a unique reduced mechanism. To quantify the difference between two mechanisms, we calculate the hamming distance between the corresponding binary vectors, which is the number of positions for which the corresponding coordinates are different. The hamming distances between every two consecutive mechanisms for 99% cutoff are represented in Fig. 12. As we can see in Fig. 12, the hamming distance between two consecutive mechanisms are less than 10% of the reduced mechanism sizes. While in the adaptive scheme proposed in our previous work (He et al., 2008) where 30 pre-developed reduced mechanisms were used, the hamming distance between two consecutive mechanisms was 26 on average. It was observed in our previous work that slower integration or even ODE solver failure was induced at the mechanism switching point. This is because discontinuity on species conversion rates is induced when two different mechanisms are used before and after the switching point. The gap between two evaluations may cause more iterations in the ODE solver. When the gap is too large for the

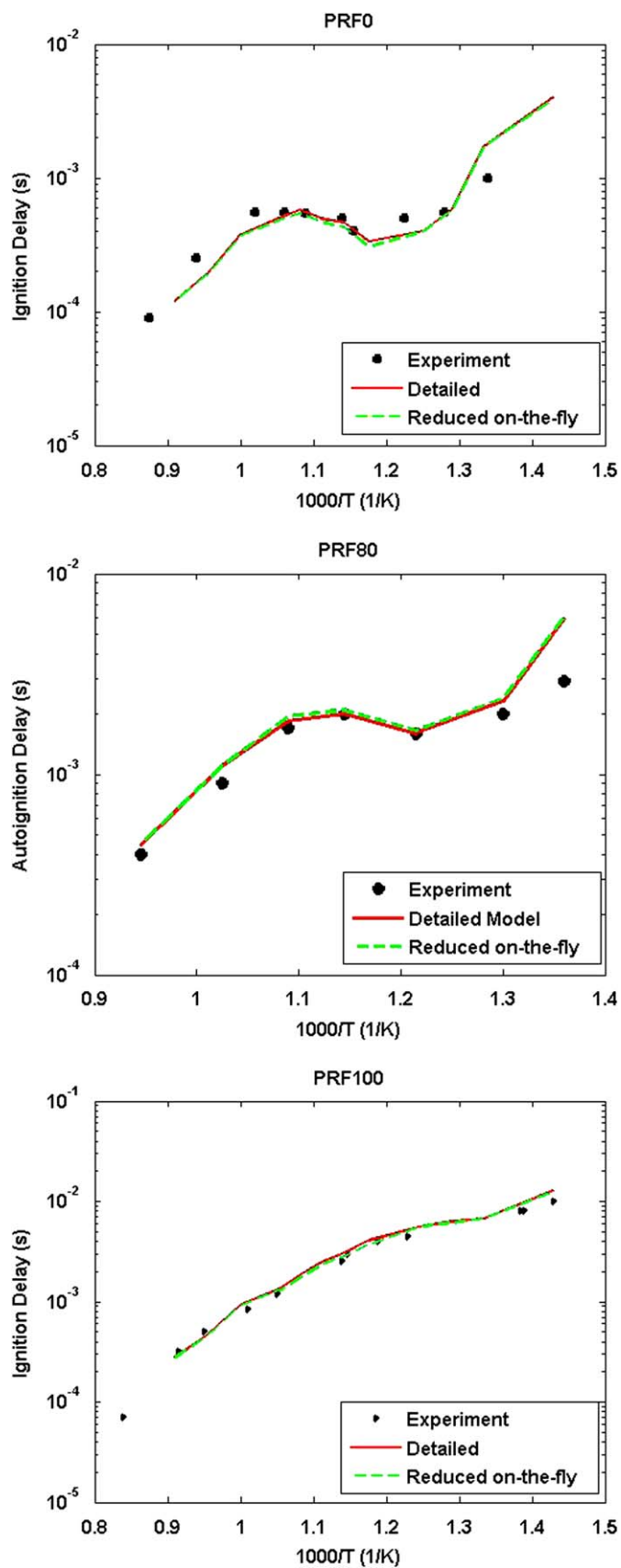


Fig. 13. Autoignition delay times of primary reference fuels with different octane numbers. The 99% cutoff was used in the on-the-fly scheme. Stoichiometric fuel/air mixture was used in all simulations.

integration to converge, the solver may fail. By updating mechanisms frequently in current on-the-fly scheme, discontinuity between mechanisms has been reduced to a very low level. This reduces CPU time spent on solving ODE's and lowers the possibility of ODE solver failure.

The detailed PRF mechanism is also tested in PFR model to simulate the autoignition delays in the shock-tube experiments of Fieweger et al. (1997). ONO, ON80 and ON100 are tested in the simulations and the results are plotted in Figs. 13. The 99% cutoff was used in the on-the-fly scheme and stoichiometric fuel/air mixture was used as initial feed. Good agreement has been observed between predicted and experimental autoignition delay times for pure n-heptane (ONO), ON80 mixture, and pure iso-octane (ON100). The negative temperature coefficient (NTC) regions are well simulated by the detailed mechanism and on-the-fly reduction scheme. As the octane number increases, which means the volume fraction of less reactive iso-octane increases, greater autoignition delay times of PRF mixture can be observed in both the experimental and simulated results.

5. Discussions

The present work proposed an on-the-fly mechanism reduction approach to analyze and reduce complex kinetic mechanisms dynamically during CFD computation. The on-the-fly scheme is demonstrated for n-pentane and PRF combustion processes in PMSR and PFR. Both the temperature and species profiles and autoignition delays by the on-the-fly scheme exhibit excellent agreement with those obtained from detailed simulation. Meanwhile, PRF autoignition delay times predicted by the on-the-fly scheme agree with the detailed simulation and experimental results very well. Besides, four novel aspects of this approach should be emphasized:

- (1) No prior information or analysis is necessary for the proposed approach. Instead of developing a single skeletal mechanism or a reduced mechanism library which can only cover limited reactive conditions, the proposed scheme analyzes the reaction system and updates the reduced mechanism dynamically (*on-the-fly*) during the simulation. Thus locally accurate mechanisms can be developed for any condition encountered in the flow simulation. This enables the implementation of the proposed scheme in systems where no *a priori* information is available condition space.
- (2) A searching algorithm is not required to implement the on-the-fly reduction scheme in reactive flow calculations. In most adaptive reduction approaches, in order to incorporate the reduced mechanisms in the flow simulation, a high-dimensional searching algorithm is needed in order to assign to the new query points appropriate mechanisms. In the present work, since reduced mechanisms are developed dynamically for the specific time point and conditions, no searching algorithm is needed and the relevant computational overhead is avoided.
- (3) Discontinuity in species conversion rates is reduced by using the on-the-fly reduction scheme which results in smaller difference between two consecutive mechanisms. In adaptive reduction scheme, the simulation switches from one reduced mechanism to another as the reactive condition changes. Thus, the conversion rates of species are evaluated based on different reaction sets before and after the switching point, which may cause discontinuity at the switching point. Based on our previous experience, the discontinuity in species integration may cause species composition oscillation, which increases the computational complexity or even causes failure

on the ODE solver. In the present work, the reduced mechanisms are developed on the fly and the difference between two consecutive mechanisms is very small. The small difference between two consecutive mechanisms minimizes the discontinuity on species conversion rates when switching mechanisms during the simulation, thus reduces the computational complexity and ensures a smooth evolution of the reaction system. However, the discontinuity of chemistry calculation in the on-the-fly scheme was not eliminated, and thus deserves more investigation in our future work.

- (4) This user-selected cutoff value is a critical parameter that can be used to define different levels of mechanism complexity: high cutoff values retain more species in the reduced mechanism thus provide more accurate simulations while low cutoff values retain less species in the reduced mechanism and more CPU time can be saved. In this work, different cutoff values have been used and the results have been compared. Based on our investigation, 99% would be appropriate for hydrocarbon combustion systems. However, when the proposed methodology is applied on other systems, cutoff value should be determined based on existing experience or preliminary study.

Acknowledgments

The authors gratefully acknowledge financial support from ExxonMobil Research & Engineering Co., NSF CBET Grant 0730582, and ONR Contract N00014-06-10835.

References

- Androulakis, I.P., 2000. Kinetic mechanism reduction based on an integer programming approach. *A.I.Ch.E. Journal* 46 (2), 361–371.
- Androulakis, I.P., Grenda, J.M., Bozzelli, J.W., 2004. Time-integrated pointers for enabling the analysis of detailed reaction mechanisms. *A.I.Ch.E. Journal* 50 (11), 2956–2970.
- Bhattacharjee, B., Schwer, D.A., Barton, P.I., Green, W.H., 2003. Optimally-reduced kinetic models: reaction elimination in large-scale kinetic mechanisms. *Combustion and Flame* 135 (3), 191–208.
- Chen, J.Y., 1988. A general procedure for constructing reduced reaction mechanisms with given independent reactions. *Combustion Science Techniques* 57, 89–94.
- Curran, H.J., Gaffuri, P., Pitz, W.J., Westbrook, C.K., 1998. A comprehensive modeling study of n-heptane oxidation. *Combustion and Flame* 114 (1–2), 149–177.
- Faravelli, T., Bua, L., Frassoldati, A., Antifora, A., Tognotti, L., Ranzi, E., 2001. A new procedure for predicting NO_x emissions from furnaces. *Computers & Chemical Engineering* 25 (4–6), 613–618.
- Fieweger, K., Blumenthal, R., Adomeit, G., 1997. Self-ignition of SI engine model fuels: a shock tube investigation at high pressure. *Combustion and Flame* 109 (4), 599–619.
- Granata, S., Faravelli, T., Ranzi, E., Olten, N., Senkan, S., 2002. Kinetic modeling of counterflow diffusion flames of butadiene. *Combustion and Flame* 131 (3), 273–284.
- He, K., Ierapetritou, M.G., Androulakis, I.P., 2008. A graph-based approach to developing adaptive representations of complex reaction mechanisms. *Combustion and Flame* 155 (4), 585–604.
- Kaper, H.G., Kaper, T.J., 2002. Asymptotic analysis of two reduction methods for systems of chemical reactions. *Physica D* 165 (1–2), 66–93.
- Kee, R.J., Rupley, F.M., Meeks, E., Miller, J.A., 1996. CHEMKIN-III: A FORTRAN Chemical Kinetics Package for the Analysis of Gas-phase Chemical and Plasma Kinetics. Sandia National Labs, Livermore, CA (United States).
- Kuo, J., Wei, J., 1969. A lumping analysis in monomolecular reaction systems. *Analysis of exactly lumpable systems. Industrial & Engineering Chemistry Fundamentals* 8 (1), 114–123.
- Lam, S.H., Goussis, D.A., 1994. The Csp method for simplifying kinetics. *International Journal of Chemical Kinetics* 26 (4), 461–486.
- Liang, L., Stevens, J.G., Farrell, J.T., 2008. A dynamic adaptive chemistry scheme for reactive flow computations. In: 32nd International Symposium on Combustion: in Production Progress.
- Lindstedt, R.P., Meyer, M.P., 2003. A dimensionally reduced reaction mechanism for methanol oxidation. *Proceedings of the Combustion Institute* 29, 1395–1402.
- Lu, T.F., Ju, Y.G., Law, C.K., 2001. Complex CSP for chemistry reduction and analysis. *Combustion and Flame* 126 (1–2), 1445–1455.
- Lu, T.F., Law, C.K., 2005. A directed relation graph method for mechanism reduction. *Proceedings of the Combustion Institute* 30, 1333–1341.

- Mass, U., Pope, S.B., 1992. Simplifying chemical kinetics: intrinsic low dimensional manifold in composition space. *Combustion and Flame* 88, 239–264.
- Peters, N., 1988. Systematic reduction of flame kinetics—principles and details. In: 11th International Colloquium on Dynamics of Explosions and Reactive Systems, Warsaw, Poland.
- Petzold, L., Zhu, W.J., 1999. Model reduction for chemical kinetics: an optimization approach. *A.I.Ch.E. Journal* 45 (4), 869–886.
- Pope, S.B., 1997. Computationally efficient implementation of combustion chemistry using in situ adaptive tabulation. *Combustion Theory and Modelling* 1 (1), 41–63.
- Rabitz, H., Kramer, M., Dacol, D., 1983. Sensitivity analysis in chemical kinetics. *Annual Review of Physical Chemistry* 34, 419–461.
- Revel, J., Boettner, J.C., Cathonnet, M., Bachman, J.S., 1994. Derivation of a global chemical kinetic mechanism for methane ignition and combustion. *Journal De Chimie Physique Et De Physico-Chimie Biologique* 91 (4), 365–382.
- Tomlin, A.S., Li, G.Y., Rabitz, H., Toth, J., 1994. A general-analysis of approximate nonlinear lumping in chemical-kinetics. 2. Constrained lumping. *Journal of Chemical Physics* 101 (2), 1188–1201.
- Turanyi, T., 1990. Reduction of large reaction mechanisms. *New Journal of Chemistry* 14, 795–803.